



Published in final edited form as:

J Neurochem. 2009 May ; 109(3): 923–934.

Functional relevance of aromatic residues in the first transmembrane domain of P2X receptors

Marie Jindrichova¹, Vojtech Vavra¹, Tomas Obsil^{1,2}, Stanko S. Stojilkovic^{3,*}, and Hana Zemkova^{1,*}

¹Department of Cellular and Molecular Neuroendocrinology, Institute of Physiology of the Academy of Sciences of the Czech Republic

²Department of Physical and Macromolecular Chemistry, Faculty of Science, Charles University, Prague, Czech Republic

³Section on Cellular Signaling, Program in Developmental Neuroscience, NICHD, NIH, Bethesda, USA

Abstract

The functional relevance of aromatic residues in the upper part of the transmembrane domain-1 of purinergic P2X receptors (P2XRs) was examined. Replacement of the conserved Tyr residue with Ala had a receptor-specific effect: the P2X1R was nonfunctional, the P2X2R, P2X4R, and P2X3R exhibited enhanced sensitivity to ATP and $\alpha\beta$ -meATP accompanied by prolonged decay of current after washout of agonists, and the P2X7R sensitivity for agonists was not affected, though decay of current was delayed. The replacement of the P2X4R-Tyr⁴² with other amino acids revealed the relevance of an aromatic residue at this position. Mutation of the neighboring Phe and ipsilateral Tyr/Trp residues, but not the contralateral Phe residue, also affected the P2X2R, P2X3R, and P2X4R function. Double mutation of ipsilateral Tyr⁴² and Trp⁴⁶ P2X4R residues restored receptor function, whereas the corresponding P2X2R double mutant was not functional. In contrast, mutation of the contralateral Phe⁴⁸ residue in the P2X4R-Y42A mutant had no effect. These results indicate that aromatic residues in the upper part of TM1 play important roles in the three-dimensional structure of the P2XRs and that they are required not only for ion conductivity but also for specificity of agonist binding and/or channel gating.

Keywords

purinergic receptors; P2XR; ATP; $\alpha\beta$ -meATP; ivermectin; gating; deactivation

Introduction

Purinergic P2X receptors (P2XRs) are an ATP-gated channel family composed of seven members, termed P2X1-7, that are organized as trimeric homomers or heteromers (Nicke et al., 1998). All subunits have two transmembrane domains (TM1 and TM2), a large extracellular loop, and intracellular N- and C- termini (Brake et al., 1994; Valera et al., 1994; Newbolt et al., 1998; Torres et al., 1998). The TM1 and the outer half of TM2 are predicted to adopt α -helical structures in activated P2X2Rs (Rassendren et al., 1997; Egan et al., 1998; Haines et al., 2001a; Haines et al., 2001b; Jiang et al., 2001; Migita et al., 2001; Li

* Author correspondence and reprint requests to: S.S.S. (stojilks@mail.nih.gov) or H.Z. (zemkova@biomed.cas.cz). Editorial correspondence should be addressed to: Dr. Hana Zemkova, Institute of Physiology, Academy of Sciences of the Czech Republic, Videnská 1083, 142 20 Prague 4, Czech Republic; Tel: 420 2 4106 2574, Fax: 420 2 4106 2488, E-mail: zemkova@biomed.cas.cz.

et al., 2004; Khakh and Egan, 2005) and P2X4Rs (Silberberg et al., 2005; Jelinkova et al., 2008), and helices of different subunits move relative to each other during channel opening and closing (Egan et al., 1998; Jiang et al., 2001; Li et al., 2004; Silberberg et al., 2005; Silberberg et al., 2007). The TM2 region appears to play a dominant role in receptor functions, including the fixation of receptors in the membrane (Torres et al., 1999; Duckwitz et al., 2006), channel assembly, gating, ion selectivity, and permeability for divalent ions (Egan et al., 1998; Migita et al., 2001; Egan and Khakh, 2004; Li et al., 2004; Khakh and Egan, 2005; Samways and Egan, 2007; Li et al., 2008). The TM2 residues Thr³³⁶, Thr³³⁹ and Ser³⁴⁰ were suggested to contribute to the formation of the pore, gate, and selectivity filter of P2X2Rs (Migita et al., 2001; Egan and Khakh, 2004; Samways and Egan, 2007; Li et al., 2008).

The accessibility rate test of TM1 cysteine mutants to water-soluble thiol-reactive compounds showed that only the V48C mutant was modified to a considerable degree in activated P2X2R. This finding was taken as evidence that the TM1 helix does not directly form the pore but is instead positioned more peripherally than TM2 (Li et al., 2008). The authors also concluded that this domain could make a significant contribution to control the ion permeability if TM1 and TM2 span the membrane at different angles (Li et al., 2008). Consistent with this idea, earlier published experiments showed that TM1 is less important for the control of ion fluxes (Jiang et al., 2003; Khakh and Egan, 2005; Samways et al., 2008); together with the TM2 domain, however, it may contribute to the control of Ca²⁺ permeability (Samways et al., 2008) and the transition of the channel pore from a relatively selective state to a dilated state (Khakh and Egan, 2005). The TM1 domain may also play a role in other receptor functions. For example, replacement of the TM1 domain of the rat P2X2 subunit with the corresponding domain from $\alpha\beta$ -meATP-sensitive P2X1 or P2X3 subunits allowed the resulting chimera to display $\alpha\beta$ -meATP sensitivity. This conversion did not occur when the TM1 domain came from a non- $\alpha\beta$ -meATP-sensitive subunit (Haines et al., 2001b).

Despite these observations, the aspects of the TM1 structure of the P2X1R and P2X3R and/or dynamics that give rise to this change in sensitivity remain unknown. Cysteine and alanine scanning mutagenesis of the P2X2R and P2X4R showed that the aromatic residues in TM1 may play an important role in receptor functions, as substitution of the conserved residue tyrosine generates a channel with enhanced sensitivity to agonists (Haines et al., 2001b; Li et al., 2004; Jelinkova et al., 2008). The upper parts of P2XR-TM1 domains are enriched with aromatic residues (Fig. 1A). In addition to the conserved tyrosine residue at the α -position, the homologous aromatic residues Trp/Tyr/Phe are conserved at the γ -position in all receptors and phenylalanine at the δ -position is present in five of seven receptors. The P2X2R and P2X3R also contain phenylalanine at the β -position. The aim of the present study was to provide a comparative view of the role of these aromatic residues in receptor function using rat P2X1R, P2X2R, P2X3R, P2X4R, and P2X7R expressed in HEK293 cells.

Material and Methods

Cells cultures and transfection

Experiments were performed on human embryonic kidney 293 cells (HEK293; American Type Culture Collection), which were grown in Dulbecco's modified Eagle's medium supplemented with 10% fetal bovine serum, 50 U/ml penicillin, and 50 μ g/ml streptomycin in a humidified 5% CO₂ atmosphere at 37°C. Cells were cultured in 75 cm² plastic culture flasks (NUNC, Rochester, NY) for 36–72 h until they reached 80–95% confluence. Before the day of transfection, ~150,000 cells were plated on 35 mm culture dishes (Sarstedt, Newton, NC) with three 12 mm poly-L-lysine-coated coverslips (Glaswarenfabrik Karl

Hecht KG, Sandheim, Germany) and incubated at 37°C for at least 24 h. For each culture dish of HEK293 cells, transfection of either wild type or mutant receptors was conducted using 1 µg of DNA and 7 µl of Lipofectamine 2000 in 2 ml of serum-free Opti-MEM according to manufacturer's instructions (Invitrogen, UK or Carlsbad, CA, USA). After 6 h of incubation, the transfection mixture was replaced with Dulbecco's modified Eagle's medium and cultured for an additional 24–48 h. Transfected cells were identified by the fluorescence signal of GFP using an inverted research microscope with fluorescence illuminators (Model IX71; Olympus, Melville, NY).

DNA constructs

cDNAs encoding the sequences of the rat P2X1, P2X2, P2X3, P2X4, P2X7, and mutated subunits were subcloned into the bicistronic enhanced fluorescent protein expression vector pIRES2-EGFP (Clontech, Mountain View, CA, USA). Mutagenesis (QuikChange site-directed mutagenesis kit; Stratagene, La Jolla, CA) was performed using P2X/pIRES2-EGFP as the template with oligonucleotides (synthesized by VBC-Genomics, Vienna, Austria) introducing specific point mutations. The C-terminal EGFP-tagged P2X4 construct was also used for mutagenesis. Previous experiments showed that this receptor responds to ATP with a sensitivity and peak amplitude of current highly comparable to those observed in cells expressing the non-tagged WT receptor (Yan et al., 2005). Plasmid DNAs for transfection were purified using a Jetquick plasmid spin kit (Genomed, Löhne, Germany). The presence of the mutations and the identity of all constructs were verified by dye terminator cycle sequencing (PerkinElmer Life and Analytical Sciences, Boston MA - performed by the Laboratory of Molecular Technology, NCI, Frederick, MD and Veritas, Inc. Rockville, MD; ABI PRISM 3100, Applied Biosystems, Foster City, CA - performed by the Laboratory of DNA sequencing, Institute of Microbiology, ASCR, Prague).

Localization of EGFP-tagged receptors

Transiently transfected HEK293 cells with P2X4-WT receptor and its mutants were plated onto 12 mm poly-L-lysine-coated coverslips and cultured in Opti-MEM supplemented with 5% fetal calf serum in a water-saturated atmosphere of 5% CO₂ and 95% air at 37°C. The following day, cells were fixed in ice-cold 4% paraformaldehyde (pH 7.4) in PBS for 5 min, dehydrated through ascending series of ethanol (70%, 80%, 95%, 1 min in each) and then coverslips mounted in Vectashield medium (Vector Laboratories, Burlingame, CA) onto glass slides. The localization of EGFP-tagged P2X4 receptors in cells was examined by laser scanning confocal microscopy (Leica SP2 AOBS, Germany). Images were collected under 60x objective lens with further zoom applied.

Immunocytochemistry

To test the presence of P2X1R proteins in the membrane, after fixation cells were incubated overnight with primary rabbit anti-P2X1R antibody 1:1000 (Alomone Laboratories, Jerusalem, Israel), in Tris buffered saline (0.05M; pH 7.6) containing 0.1% TritonX-100 and 5% fetal calf serum at 4°C. The preparations were washed three times for 5 min in the same buffer and then incubated with secondary antibody Cy5-conjugated goat anti-rabbit IgG (Chemicon International, Inc., Temecula, CA). After intensive washing, the cultures were dehydrated and covered with Vectashield medium.

Patch clamp recordings

Currents were recorded in a whole-cell configuration from cells clamped to –60 mV using an Axopatch 200B patch-clamp amplifier (Axon Instruments, Union City, CA). Records were captured and stored using Digidata 1322A and pClamp9 software package. Patch electrodes were pulled from a glass tube with a 1.65 mm outer diameter on a horizontal

puller (Sutter, USA). The tip of the pipette was heat-polished and its resistance was 3–5 M Ω . Whole-cell recording was performed using 40–60% series resistance compensation. During the experiments, the coverslip with cell culture was transferred into a recording chamber, which was continuously perfused with an extracellular solution containing (in mM): 142 NaCl, 3 KCl, 2 CaCl₂, 1 MgCl₂, 10 HEPES and 10 D-glucose, adjusted to pH 7.3 with 1M NaOH. The osmolarity of the solution was 290 – 300 mOsm as determined by a vapor pressure osmometer (Model VAPRO 5520; Wescor, Logan, UT). Patch electrodes used for whole-cell recording were filled with an intracellular solution containing (in mM): 154 CsCl, EGTA 11, and HEPES 10; pH was adjusted with 1 M CsOH to 7.2. The osmolarity of the intracellular solution was 280 – 290 mOsm. Ivermectin (IVM) was dissolved in DMSO, stored in stock solutions at 10 mM, and diluted to required concentration in extracellular solution prior to experiments. Control and ATP-containing solutions were applied using RSC-200 Rapid Solution Changer system (BIO-LOGIC, Claix, France); less than 100 ms was required for exchange of solutions around the patched cell. For stimulation of cells expressing P2X1R, an Ultrafast Solution-Switching System (LSS-3200; EXFO Burleigh Products Group Inc., Victor, NY) was used that was simultaneously program-controlled by pClamp9 software through PZ-150M Amplifier; and exchange of solutions was set within 5 ms. Brief (2–4 s duration, 2–4 min interval) application of different concentrations of agonists was used to evoke inward current; one or two responses were recorded from one cell per coverslip. To estimate the EC₅₀ values, the responses from 15–50 different cells were pooled and dose response curves were constructed using mean values.

Calculations

Dose-response data points were fitted by a three-parameter logistic equation using a nonlinear curve-fitting program that derives the EC₅₀ and Hill coefficient values of the produced curves (SigmaPlot 2000 v9.01; SPSS Inc., Chicago, IL). The form of the fitted equation was $y = I_{max} / (1 + (EC_{50}/x)^{n_H})$, where y is the amplitude of the current evoked by ATP (in all cases normalized), I_{max} is the maximum current amplitude induced by 100 μ M ATP, EC₅₀ is the agonist concentration producing 50% of the maximal response, n_H is the Hill coefficient, and x is the concentration of ATP. The kinetics of current decay evoked by washout of agonists, termed deactivation, were fitted by a single exponential function [$y = A_1 \exp(-t/\tau)$] or by the sum of two exponentials [$y = A_1 \exp(-t/\tau_1) + A_2 \exp(-t/\tau_2)$] using the program CLAMPFIT 9 (Axon Instruments), where A_1 and A_2 are relative amplitudes of the first and second exponential, and τ_1 and τ_2 are time constants. The derived time constant for deactivation was labeled as τ_{off} . All numerical values in the text are reported as mean \pm SEM. Significant differences between means were determined by one-way analysis of variance using SigmaStat 2000 v9.01 and Tukey's post hoc test, with $P < 0.01$.

Helical wheel plot and three-dimensional modeling

The TM1 domain of P2X4 sequences was modeled as an α -helix using the DeepView/Swiss-PdbViewer v3.7 program (Guex and Peitsch, 1997) (Figs. 1 and 7).

Results

1. Alanine scanning mutagenesis of the P2X4R-TM1 domain

Scanning mutagenesis provides a systematic method for the identification of residues of potential relevance for receptor organization and function (Akabas et al., 1992). Here, we used alanine-scanning mutagenesis of the P2X4R-TM1 domain (Fig. 1A) to identify amino acids of relevance to P2XR receptor function, specifically those related to agonist potency and rate of receptor deactivation. Scanning started with the Gly²⁹ residue and ended with Trp⁵⁰. In the cases of Ala³⁴ and Ala⁴¹, we used substitutions with Phe and Leu, respectively.

The wild type (WT) and mutant receptors were expressed in HEK293 cells, and whole-cell recording of ATP-induced currents was used to measure the following parameters of receptor activity in the presence or absence of 3 μM IVM: the concentration of agonist inducing a half-maximal effect (EC_{50}), the peak current amplitude in response to a supramaximal agonist concentration (I_{max}), and the rate of decay of the current (τ_{off}) after washout of a non-desensitizing concentration of agonist. The results of these investigations are summarized in Supplemental Table 1.

The following P2X4R mutants showed no significant changes in receptor function with regard to the sensitivity to ATP and I_{max} values in the presence or absence of IVM in comparison to the P2X4R-WT: L30A, N32A, A34F, V35A, L37A, L38A, I39A, A41L, I44A, W46A, and F48A. In the absence of IVM, receptor function was also unaffected in L40A, V43A, V47A, and W50A mutants. However, these receptors showed significant changes in the EC_{50} values for ATP and deactivation kinetics in the presence of IVM in comparison to the P2X4R-WT (Supplemental Table 1). The same four residues were also identified as IVM-sensitive hits in our previous experiments with cysteine mutants (Jelinkova et al., 2008), supporting the helical organization of the upper part of the TM1 domain in activated receptors and the potential role of these residues in IVM binding. The Q36C mutant was also recognized previously as an IVM-sensitive mutant (Jelinkova et al., 2008). In contrast, the Q36A was a low-response mutant, and IVM only partially rescued the receptor's function.

Receptor functions were significantly affected in the following mutants: G29A, M31A, R33A, Y42A, G45A, and V49A. The V49A and R33A mutants responded to ATP application with small I_{max} values, and their EC_{50} s could not be determined. The receptor function of these mutants was partially rescued by IVM treatment. The G29A and M31A receptors were functional, but less sensitive to ATP than P2X4R-WT, and IVM treatment fully restored the function of these mutants (Supplemental Table 1). In contrast to the complete or partial loss of ATP sensitivity for these four mutants, the G45A and Y42A mutants showed enhanced sensitivity to the agonist as indicated by the leftward shifts in their EC_{50} values. The IVM treatment further sensitized the G45A but not Y42A mutant, suggesting that the latter receptor was maximally sensitized. The EC_{50} values for ATP in the absence and presence of IVM for Y42A mutant were identical ($0.6 \pm 0.1 \mu\text{M}$), and the receptor deactivated with a τ_{off} of 24 ± 2.9 s in the absence of IVM and 29 ± 4.4 s in the presence of IVM. Receptor function was also affected in terms of the amplitude of I_{max} and the inability of IVM to increase it. Among these six residues, Gly²⁹ and Tyr⁴² are completely conserved, and Arg³³ and Gly⁴⁵ are present in four of seven rat P2XRs. Val⁴⁹ is also present in the P2X1R, and Met³¹ is unique for the P2X4R (Fig. 1A). The relevance of these six residues for receptor function was also supported by the finding that their replacement with cysteine resulted in comparable changes (Jelinkova et al., 2008).

2. Effect of substitution of the conserved tyrosine TM-1 residue on P2XR function

In further work, we focused on the conserved tyrosine residue at the α -position and several other aromatic residues in the upper part of the P2XR-TM1 domain (Fig. 1A, positions β , γ , and δ). The locations of these residues in the predicted α -helical P2XR-TM1 segments are shown in Fig. 1B. The conserved TM1 tyrosine residue was replaced with alanine in P2X4R, P2X1R, P2X2R, P2X3R, and P2X7R; the function of these mutants was then examined. All receptors, including the non-functional P2X1-Y43A mutant (Fig. 2A, top panel), were expressed in the plasma membrane (Fig. 2B). The P2X2R, P2X3R, and P2X4R mutants were functional but they did respond to a supramaximal concentration of agonists (100 μM ATP for P2X2 and P2X4 and 10 μM ATP for P2X3 mutants) with significantly lower I_{max} values than WT receptors (Table 1). The P2X7R mutant was also functional and responded to 300 μM BzATP with a lower I_{max} (WT = 2.0 ± 0.3 nA; P2X7-Y40A = 0.47 ± 0.05 nA).

The decay of current in cells expressing the wild type P2X2R, P2X3R, and P2X4R was rapid and monophasic; in contrast wild type P2X7R deactivated bi-exponentially. The decay of currents after washout of agonists was significantly delayed in all functional α -mutants (Fig. 2A, Table 1), suggesting a common role of the aromatic residue at this position for all receptors. The deactivation kinetics of the P2X2R and P2X4R α -mutants was also monophasic; however, the delay in receptor deactivation was more profound in cells expressing the P2X4-Y42A mutant than the P2X2-Y43A receptors. In cells expressing the P2X3-Y37A mutant, the decay of current was biphasic. The mean value of the fast decay component was comparable to the P2X3R-WT τ_{off} , while the slow decay component, which contributed 36% of the current decay, was comparable to the τ_{off} of the P2X4-Y42A mutant (Table 1). Repeated stimulation of cells expressing P2X3R-WT with high ATP concentrations using intervals of 4 minutes or shorter between applications resulted in a progressive decrease in current peak amplitude, indicating that, in part, decay of current reflects desensitization of receptors (supplemental Fig. 1, top panels). However, the amplitudes of P2X3-Y37A current were comparable during repetitive stimulation, suggesting that the second phase of current decay may reflect accelerated return from the desensitized to the open state (supplemental Fig. 1, bottom traces). The kinetics of the P2X7-Y40A mutant current decay was bi-exponential, and the participation of the slow decay component was higher in mutant receptors ($81 \pm 4\%$) than in P2X7-WT receptors ($33 \pm 6\%$).

We also measured the sensitivity of the WT and α -P2X mutants to agonists. Under our experimental conditions, the potency of ATP for P2X2R-WT and P2X4R-WT was comparable, with estimated EC_{50} values of $5.4 \mu\text{M}$ and $4.6 \mu\text{M}$, respectively. In contrast, the EC_{50} value for ATP for the P2X3R-WT was $0.35 \mu\text{M}$. Replacement of the conserved tyrosine in these three receptors resulted in roughly 20-, 8-, and 2-fold decreases in the EC_{50} values for ATP for the P2X2-Y43A, P2X4-Y42A, and P2X3-Y37A mutants, respectively (Table 1; Fig. 3A–C, left panels). The splice form of the P2X2R, termed P2X2bR (Lynch et al., 1999), also exhibited an increase in sensitivity to ATP that was comparable to that observed in cells expressing the full-size receptor (data not shown). In contrast, the P2X7-WT and P2X7-Y40A mutant exhibited equipotent sensitivity to BzATP over a 30–300 μM concentration range, with EC_{50} values of $29 \mu\text{M}$ and $20 \mu\text{M}$, respectively (Fig. 3D, left), and sensitivity to ATP was also unchanged (Fig. 3D, right).

It is well established that $\alpha\beta$ -meATP is a partial agonist for the P2X2R and P2X4R, in contrast to the P2X1R and P2X3R (Ralevic and Burnstock, 1998). Consistent with this, we observed that the P2X2R-WT responded to $\alpha\beta$ -meATP application only at higher concentrations; its EC_{50} value could thus not be estimated (Fig. 3A, right). $\alpha\beta$ -meATP sensitivity of the P2X4R-WT was also low, with an estimated EC_{50} value of $57 \mu\text{M}$ (Table 1; Fig. 3C). The $\alpha\beta$ -meATP efficacy was low, roughly 40% of that observed in response to ATP (100%). Tyrosine-to-alanine substitutions increased the potency of $\alpha\beta$ -meATP for the P2X2R and P2X4R, generating estimated EC_{50} values of $8.2 \mu\text{M}$ and $0.6 \mu\text{M}$, respectively. The latter value is comparable to that observed in cells expressing the P2X3R-WT. The efficacy of $\alpha\beta$ -meATP for the P2X2-Y43A and P2X4-Y42A mutants was greatly elevated and was equivalent to that observed with ATP, suggesting that $\alpha\beta$ -meATP is a full agonist for these mutants. A small increase in the sensitivity of the P2X3-Y37A mutant was also observed (Fig. 3B, right). These results indicate that alanine substitution of the conserved TM1 tyrosine residues had the most profound effects on the potency of agonists at the P2X2R and P2X4R, was less effective at the P2X3R, and was practically ineffective at the P2X7R.

3. Phe and Trp residues can partially substitute for Tyr at the 42 position of the P2X4R

In further experiments, we investigated which amino acid residues can substitute for the Tyr⁴² in the P2X4R. To do this, we generated eight mutants using alanine, isoleucine, cysteine, glycine, phenylalanine, tryptophan, arginine, and aspartic acid as substitute residues. The introduction of the charged residues (P2X4-Y42D and P2X4-Y42R mutants) resulted in non-functional mutants, although receptors were expressed in the plasma membrane (Fig. 4C). All other mutants were functional but exhibited significant changes in deactivation kinetics. The greatest changes occurred when Tyr⁴² was replaced with the small, uncharged amino acids glycine, isoleucine, or cysteine or the previously shown Ala substitution, with the rates of receptor deactivation in the following order: Y42G > Y42I > Y42A > Y42C (Fig. 4A). When the aromatic amino acids phenylalanine and tryptophan were used as substitutes, deactivation was faster. A logarithmic plot showed an inverse relationship between the τ_{off} and EC₅₀ values for ATP for these mutants (Fig. 4B). These results indicate that changes in volume (alanine, cysteine, isoleucine, and glycine) at the position of the conserved tyrosine residue in TM1 affect P2X4R function, but that changes in hydrophobicity (phenylalanine and tryptophan) at this position do not. Furthermore, the introduction of charged residues blocks the receptor's function. We also generated the P2X2-Y43F mutant, the deactivation time-courses and sensitivities to ATP and $\alpha\beta$ -meATP of which were indistinguishable from those of the WT-P2X2R (Table 1).

4. Effect of substitution of other aromatic TM1 residues on P2XR function

Next we tested whether the effects of replacement of the conserved tyrosine residue with alanine were specific for this residue by generating alanine mutants of aromatic residues at positions β , γ , and δ (Fig. 1A) for three receptors: the P2X2R (F44A, Y47A and F49A), P2X3R (F38A, W41A, and F43A), and P2X4R (W46A and F48A), as well as the receptor-specific mutant P2X4-W50A. We then characterized their EC₅₀ values for ATP and $\alpha\beta$ -meATP and their time courses of deactivation in response to the application of non-desensitizing ATP concentrations (Fig. 5, Table 1). All mutants were functional. Alanine substitution of Phe at the δ -position had only a minor effect on all receptors, and the P2X4-W50A mutant was normal as well (Fig. 5B–D, Table 1). In contrast, other mutants showed altered responses. The P2X2-F44A and P2X3-F38A mutants exhibited small but significant changes in the rate of receptor deactivation (Table 1, supplemental Fig. 2), and the P2X3-F38A mutant desensitized more rapidly (data not shown). Furthermore, the majority of mutants responded to supramaximal ATP stimulation with reduced current amplitude, an effect comparable to that observed in α -mutants (Fig. 5A). Mutations of residues at the β -position of the P2X2R (Fig. 5B) but not P2X3R (Fig. 5C) also mimicked the effects of mutation of conserved tyrosine residue on the potency of ATP and $\alpha\beta$ -meATP. An increase in the potency of agonists was also observed in cells expressing γ -type mutants of the P2X2R and P2X4R; the P2X2-Y47A mutant exhibited enhanced sensitivity to both ATP (about 7 fold) and $\alpha\beta$ -meATP, whereas the P2X4-W46A mutant was more sensitive to $\alpha\beta$ -meATP (Fig. 5B&D). These results demonstrate the receptor-specific role of aromatic residues at positions β and γ but not δ on agonist potency.

5. Effect of double-point TM1 alanine mutants on receptor functions

In order to study the dependence of α mutation-induced changes in P2XR function on the presence of other aromatic and nonaromatic residues in the upper TM1 domain, we generated several P2X2R and P2X4R mutants. The double-point mutants of the P2X2R (Y43A+Y47A and Y43A+F44A) were nonfunctional, suggesting that these residues are critical for receptor function. In contrast, all P2X4R double point mutants were functional. The delay in receptor deactivation induced by replacing the Tyr⁴² residue with alanine was abolished in Y42A+W46A and Y42A+W50A double mutants (Table 1; Fig. 6). These two mutants also showed enhanced I_{max} values and reduced sensitivity to ATP and $\alpha\beta$ -meATP in

comparison to the P2X4-Y42A mutant (Table 1). In further contrast to the single Y42A mutant, these double-point mutants were also sensitive to IVM (in the presence of IVM, the I_{max} increased about 1.8 fold, and τ_{off} was prolonged from 1.4 s to 11 s). Thus, receptor function was almost completely rescued by these two double aromatic residue mutants. That was not the case with the Y42A+F48A double-point mutant, the functional properties of which, including deactivation kinetics, were highly comparable to those observed in cells expressing the single-point Y42A mutant (Table 1, Fig. 6). We also substituted four non-aromatic TM1 residues in combination with the conserved Tyr⁴² at the P2X4R: Val⁴³, Ile³⁹, Val³⁵, and Gly²⁹. None of these double-point mutants further altered the P2X4-Y42A receptor function (Table 1). Analysis of the position of the alanines that were substituted for aromatic residues in the predicted helical model of the P2X4R-TM1 revealed that the effects of alanine substitution of the Tyr⁴² residue could be suppressed by alanine substitution of another aromatic residue on the ipsilateral side of TM1 helix (Trp⁴⁶ and Trp⁵⁰) but not by the substitution of residues facing the contralateral wall of the helix (Phe⁴⁸) (Fig. 6).

Discussion

The roles of aromatic TM1 residues in receptor function have been analyzed in the P2X2R and P2X4R, but not in other P2XRs. Most prior experiments have focused on the conserved tyrosine residue at the α -position. Substitution of this residue with cysteine in the P2X2R resulted in a non-functional channel (Haines et al., 2001b; Jiang et al., 2001; Li et al., 2008). On the other hand, the Y43A mutant of this receptor was described as a channel with a roughly 10-fold increased sensitivity for ATP (Li et al., 2004). Further characterization of this mutant revealed that the permeability of its channel to NMDG was reduced and that the ATP-evoked current was significantly smaller than that of the P2X2R-WT (Khakh and Egan, 2005). Recently, Egan's group reported that the P2X2-Y43A mutant showed attenuated Ca²⁺ permeability and that receptor function was not rescued by the replacement of tyrosine with phenylalanine, suggesting that these effects could reflect interactions of the hydroxyl group of tyrosine with calcium (Samways et al., 2008). Increased ATP potency (roughly 8-fold) was also observed for the P2X4-Y42W mutant, tryptophan scanning mutagenesis on TM1 of the P2X4-channel predicts that this residue may be involved in a protein-protein interaction that stabilizes the closed conformation of the channel (Silberberg et al., 2005). Consistent with this conclusion, the helical wheel projection of TM1 showed that the conserved tyrosine residue is localized on the opposite side of the lipid-oriented/IVM-sensitive residues (Jelinkova et al., 2008).

Our experiments with the P2X4R also indicated that replacing the Tyr⁴² residue with cysteine (Jelinkova et al., 2008) and alanine (present data) generates a mutant with increased sensitivity to ATP (about 8 fold) and decreased I_{max} values. In the P2X1R, replacement of this residue with alanine resulted in a non-functional channel and further supporting the importance of this residue in the receptor's function. The sensitivity of the P2X3R-Y37A mutant to ATP also increased (about 2 fold), and the I_{max} value decreased. We also observed dramatic differences in the sensitivity of the P2X2R and P2X4R tyrosine mutants to $\alpha\beta$ -meATP as well as a transition from partial to full agonist for these two receptors. For the P2X3R-WT, $\alpha\beta$ -meATP is a full agonist; its Y37A mutant showed a small decrease in the EC₅₀ value. These findings suggest that the conserved TM1 tyrosine plays an important role in agonist binding and/or channel gating. This was only partially the case with the P2X7R mutant, which did not show gain in sensitivity to ATP in our experimental conditions, but did exhibit altered deactivation kinetics. Others suggested that the ectodomain of this receptor is solely responsible for agonist potency (Young et al., 2007). The reason for the difference between P2X7R and other P2XRs could also be related to its structure (longer C-terminal), distribution of TM1 aromatic residues, integration of pannexin-1 channels into

signaling (Pelegrin and Surprenant, 2006), or specific gating properties (rapid opening of an integral channel pore followed by pore dilation) (Yan et al., 2008).

Changes in agonist selectivity and potency for the P2XR generated by introducing the alanine mutation at α -position also had a strong effect on the rate of decay of current after washout of the agonist. In general, the enhanced sensitivity of receptors to agonists should reflect (at least in part) on the rates of receptor deactivation after the washout of ATP. The P2X4-Y42A mutation practically mimicked the effect of IVM, a drug that appears to increase the frequency of channel openings (Priel and Silberberg, 2004), greatly enhance the sensitivity of a receptor to agonists, and delay deactivation of receptors through direct interactions with TMs (Jelinkova et al., 2006; Silberberg et al., 2007; Jelinkova et al., 2008). Thus, it is reasonable to suggest that the frequency of opening is high for the P2X4-Y42A mutant and cannot be further increased by IVM. Substitutions of various amino acids for tyrosine at position 42 of the P2X4R showed that an aromatic residue is required at this position for normal receptor function. The increase in the sensitivity of the P2X2R mutant for agonists could also provide a rationale for delay in washout kinetics.

On the other hand, small changes in agonist sensitivity for the P2X3-Y37A mutant were accompanied by a significant delay in washout kinetics and shift from monophasic to biphasic decay of current. Experiments with repetitive agonist applications suggested that the second phase in current decay may reflect accelerated return from the desensitized to the open state, but further experiments are required to test this hypothesis. Finally, although the P2X7R mutant did not show an obvious increase in sensitivity to agonist, it exhibited greatly reduced maximum amplitude and delay in decay of current after washout of agonists, the latter reflecting an increase in the contribution of the second component of decay. This could not be explained by the recovery from desensitization state because the P2X7R does not desensitize. However, our ongoing experiments revealed that two phases in decay of P2X7R current reflect transition from dilated to open state (rapid component) and from open to closed state (slow component) (Yan and Stojilkovic, unpublished), findings consistent with the two distinct ATP activation sites at the P2X7R (Klapperstuck et al., 2001). This could indicate that the α -mutant of P2X7R shows altered rates of receptor dilation, which in turn affects deactivation kinetics.

Previous reports describe a point mutation conferring sensitivity to $\alpha\beta$ -meATP and the slowing of P2X2R deactivation via the mutation of the neighboring aromatic residue Phe⁴⁴ (Jiang et al., 2001; Haines et al., 2001b). Both alanine and cysteine substitutions of this residue also confer enhanced sensitivity to ATP, with EC₅₀ values of 0.3 – 0.7 μ M (Li et al., 2004; Li et al., 2008) as well as slightly prolonged deactivation time constants (to 1.2 s) (Jiang et al., 2001). These findings are consistent with our data from the F44A mutant. In addition to the P2X2R, only the P2X3R at the β -position has an aromatic residue. Here, we show that mutation of this phenylalanine produced a prolonged deactivation without further enhancing the sensitivity of the receptor for agonists. However, the amplitude of the ATP-induced current for the P2X3-F38A receptor was very low and it desensitized rapidly, making it difficult to measure the dose-response curve. These results suggest that aromatic residues at the β -position have a similar role to that of tyrosine in the α -position in P2X2R and P2X3R function.

All P2XRs also have an aromatic residue at the γ -position. The P2X2-Y47A mutant has been previously reported to be nonfunctional (Li et al., 2004; Khakh and Egan, 2005) (Haines et al., 2001b; Samways et al., 2008), whereas the P2X2-Y47C mutant was normal (Haines et al., 2001b; Li et al., 2008). In our study, the P2X2-Y47A mutant was functional but showed a significantly lower I_{max} value. It also showed an increase in the sensitivity for ATP (about 7 fold) and $\alpha\beta$ -meATP, indicating that this substitution was less effective than

that observed in cells expressing P2X2-Y43A mutants. Mutation of aromatic residues at the γ -position of the P2X4R but not P2X3R also sensitized the receptor to $\alpha\beta$ -meATP. A similar conclusion was reached by others using the P2X4-W46A mutant (Silberberg et al., 2005). Substitution of the phenylalanine residue at the δ -position with alanine did not affect P2X2R and P2X3R functions and produced a small increase in the sensitivity of the P2X4-F48A mutant for $\alpha\beta$ -meATP but not ATP. We have reached similar conclusions in previous experiments with the P2X4-F48C mutant (Jelinkova et al., 2008). Others also observed normal receptor function of P2X2-F49A and F49C mutants (Haines et al., 2001b; Li et al., 2004; Khakh and Egan, 2005; Samways et al., 2008). Finally, mutation of this residue at the P2X4R did not reverse or potentiate effects of a single Tyr⁴² mutation on receptor function.

Our experiments with double-point mutants were designed with the purpose to analyze the impact of the position of aromatic residues in TM1 region on the receptor functions. The P2X2-Y43A+Y47A and P2X2-F44A+Y47A mutants were nonfunctional. In contrast, the deactivation and the sensitizing effects of the P2X4-Tyr⁴² mutation were reversed in Y42A+W46A and Y42A+W50A mutants, but not in the Y42A+F48A mutant. Fig. 6 shows that aromatic residues at positions 42, 46, and 50 are on the same side of the TM1 domain, whereas the Phe⁴⁸ residue is on the contralateral side. This model was based on experimental data obtained from cysteine- (Jelinkova et al., 2008) and alanine- (here) scanning mutagenesis of the rat P2X4R. These results indicate that ipsilateral aromatic residues in the P2X4R-TM region are important but not dominant, because the proper three-dimensional structure of the receptor in the resting condition, as well as conformational changes induced by agonist binding, could be achieved in their absence. For P2X2R, these residues could also be dominant.

The TM2 residues also contribute to the control of receptor sensitivity for agonists and deactivation rates. The P2X2R-TM2 residue Thr³³⁹ is likely to be close to the narrowest part of the pore at approximately the same relative distance through the membrane as TM1 Tyr⁴³ and Phe⁴⁴ (Cao et al., 2007). The P2X2-T339S mutant exhibited pronounced spontaneous channel openings and was roughly 10-fold more sensitive to ATP and $\alpha\beta$ -meATP, but this effect was not observed in K308A+T339S double-point mutants. The authors (Cao et al., 2007) concluded that Lys³⁰⁸, which has been previously suggested to contribute to agonist binding (Jiang et al., 2000), has a primary role in gating and that each mutation (i.e., T339S and K308A) has an independent effect on channel gating.

The ATP binding site in the ectodomain is probably located in the inter-subunit pocket (Wilkinson et al., 2006; Marquez-Klaka et al., 2007), indicating that substitution of TM1 aromatic residues at the interface embedded in the membrane might induce far-reaching changes in the ectodomain and affect agonist binding. Based on experiments presented here, we propose that the substitution of residues at 42, 46, and 50 positions (P2X4R numbering) may cause the displacement of a distal ATP binding pocket, which becomes more coordinated to the $\alpha\beta$ -meATP molecule in the P2X2R and P2X4R, and to a smaller extent in the P2X3R. This in turn affects the rates of receptor deactivation. It also appears that TM1 aromatic residues may affect receptor gating independently of the potency of agonists, as shown for P2X3R and P2X7R. Thus, with respect to a TM1 structure-functional relationship, it is reasonable to conclude that the P2X2R and P2X4R represent a separate subgroup of receptors.

In summary, our comparative study reveals the receptor-specific role of aromatic residues in the upper part of the TM1 helix. The conserved tyrosine residue at α -position is probably critical for P2X1R operation because its replacement with alanine resulted in a non-functional receptor. All other α -mutant receptors were functional but exhibited delay in washout kinetics. At P2X2R and P2X4R, and to a small extent at P2X3R, this mutation also

increased the sensitivity of receptors for ATP. This mutation also increased the potency and efficacy of $\alpha\beta$ -meATP for the P2X2R and P2X4R. Mutation of aromatic TM1 residues at the γ -position of the P2X2R and P2X3R had effects on receptor function that were similar to those from the replacement of the conserved TM1 tyrosine with alanine. The replacement of aromatic residues at the γ -position with alanine also resulted in altered P2X2R, P2X3R, and P2X4R functions. The TM1 aromatic residues at the δ -position are unlikely to play an important role in the potency and efficacy of agonists and activation/deactivation kinetics. Double mutation of ipsilateral aromatic P2X4R residues restored the receptor function and the corresponding P2X2R double mutant was not functional. These findings are consistent with the idea that a subset of aromatic residues in the upper part of TM1 plays an important role in the three-dimensional organization of the P2XRs and is required for agonist binding or gating. We also assume that the position of these residues on one side of the TM1 helix and the residue orientation at the interface between two different subunits are important for receptor function.

Supplementary Material

Refer to Web version on PubMed Central for supplementary material.

Abbreviations

EGFP	enhanced green fluorescent protein
HEK293	human embryonic kidney cells
EC₅₀	agonist concentration inducing half-maximal effect
I_{max}	maximum amplitude of current
IVM	Ivermectin
P2XR	P2 purinergic receptor channels
τ_{off}	deactivation time constant
$\alpha\beta$-meATP	$\alpha\beta$ -methyleneadenosine 5'-triphosphate
BzATP	2'-3'-O-(4-benzoylbenzoyl)-adenosine 5'-triphosphate.

Acknowledgments

This study was supported by the Internal Grant Agency of Academy of Sciences (Grants No. A5011408, IAA500110702 and IAA500110910), the Grant Agency of the Czech Republic (305/07/0681, the Academy of Sciences of the Czech Republic (Research Project No. AVOZ 50110509), the Centrum for Neuroscience (Research Project No. LC554), and the Intramural Research Program of the NICHD, NIH.

References

- Akabas MH, Stauffer DA, Xu M, Karlin A. Acetylcholine receptor channel structure probed in cysteine-substitution mutants. *Science*. 1992; 258:307–310. [PubMed: 1384130]
- Brake AJ, Wagenbach MJ, Julius D. New structural motif for ligand-gated ion channels defined by an ionotropic ATP receptor. *Nature*. 1994; 371:519–523. [PubMed: 7523952]
- Cao L, Young MT, Broomhead HE, Fountain SJ, North RA. Thr³³⁹-to-serine substitution in rat P2X2 receptor second transmembrane domain causes constitutive opening and indicates a gating role for Lys308. *J Neurosci*. 2007; 27:12916–12923. [PubMed: 18032665]
- Duckwitz W, Hausmann R, Aschrafi A, Schmalzing G. P2X₅ subunit assembly requires scaffolding by the second transmembrane domain and a conserved aspartate. *J Biol Chem*. 2006; 281:39561–39572. [PubMed: 17001079]

- Egan TM, Khakh BS. Contribution of calcium ions to P2X channel responses. *J Neurosci.* 2004; 24:3413–3420. [PubMed: 15056721]
- Egan TM, Haines WR, Voigt MM. A domain contributing to the ion channel of ATP-gated P2X2 receptors identified by the substituted cysteine accessibility method. *J Neurosci.* 1998; 18:2350–2359. [PubMed: 9502796]
- Guex N, Peitsch MC. SWISS-MODEL and the Swiss-PdbViewer: An environment for comparative protein modeling. *Electrophoresis.* 1997; 18:2714–2723. [PubMed: 9504803]
- Haines WR, Migita K, Cox JA, Egan TM, Voigt MM. The first transmembrane domain of the P2X receptor subunit participates in the agonist-induced gating of the channel. *J Biol Chem.* 2001a; 276:32793–32798. [PubMed: 11438537]
- Haines WR, Voigt MM, Migita K, Torres GE, Egan TM. On the contribution of the first transmembrane domain to whole-cell current through an ATP-gated ionotropic P2X receptor. *J Neurosci.* 2001b; 21:5885–5892. [PubMed: 11487611]
- Jelinkova I, Yan Z, Liang Z, Moonat S, Teisinger J, Stojilkovic SS, Zemkova H. Identification of P2X4 receptor-specific residues contributing to the ivermectin effects on channel deactivation. *Biochem Biophys Res Commun.* 2006; 349:619–625. [PubMed: 16949036]
- Jelinkova I, Vavra V, Jindrichova M, Obsil T, Zemkova HW, Zemkova H, Stojilkovic SS. Identification of P2X4 receptor transmembrane residues contributing to channel gating and interaction with ivermectin. *Pflugers Arch.* 2008; 456:939–950. [PubMed: 18427835]
- Jiang LH, Rassendren F, Surprenant A, North RA. Identification of amino acid residues contributing to the ATP-binding site of a purinergic P2X receptor. *J Biol Chem.* 2000; 275:34190–34196. [PubMed: 10940304]
- Jiang LH, Rassendren F, Spelta V, Surprenant A, North RA. Amino acid residues involved in gating identified in the first membrane-spanning domain of the rat P2X2 receptor. *J Biol Chem.* 2001; 276:14902–14908. [PubMed: 11278888]
- Jiang LH, Kim M, Spelta V, Bo X, Surprenant A, North RA. Subunit arrangement in P2X receptors. *J Neurosci.* 2003; 23:8903–8910. [PubMed: 14523092]
- Khakh BS, Egan TM. Contribution of transmembrane regions to ATP-gated P2X2 channel permeability dynamics. *J Biol Chem.* 2005; 280:6118–6129. [PubMed: 15556949]
- Klapperstuck M, Buttner C, Schmalzing G, Markwardt F. Functional evidence of distinct ATP activation sites at the human P2X(7) receptor. *J Physiol.* 2001; 534:25–35. [PubMed: 11432989]
- Li M, Chang TH, Silberberg SD, Swartz KJ. Gating the pore of P2X receptor channels. *Nat Neurosci.* 2008
- Li Z, Migita K, Samways DS, Voigt MM, Egan TM. Gain and loss of channel function by alanine substitutions in the transmembrane segments of the rat ATP-gated P2X2 receptor. *J Neurosci.* 2004; 24:7378–7386. [PubMed: 15317863]
- Lynch KJ, Touma E, Niforatos W, Kage KL, Burgard EC, van Biesen T, Kowaluk EA, Jarvis MF. Molecular and functional characterization of human P2X2 receptors. *Mol Pharmacol.* 1999; 56:1171–1181. [PubMed: 10570044]
- Marquez-Klaka B, Rettinger J, Bhargava Y, Eisele T, Nicke A. Identification of an intersubunit cross-link between substituted cysteine residues located in the putative ATP binding site of the P2X1 receptor. *J Neurosci.* 2007; 27:1456–1466. [PubMed: 17287520]
- Migita K, Haines WR, Voigt MM, Egan TM. Polar residues of the second transmembrane domain influence cation permeability of the ATP-gated P2X2 receptor. *J Biol Chem.* 2001; 276:30934–30941. [PubMed: 11402044]
- Newbolt A, Stoop R, Virginio C, Surprenant A, North RA, Buell G, Rassendren F. Membrane topology of an ATP-gated ion channel (P2X receptor). *J Biol Chem.* 1998; 273:15177–15182. [PubMed: 9614131]
- Nicke A, Baumert HG, Rettinger J, Eichele A, Lambrecht G, Mutschler E, Schmalzing G. P2X1 and P2X3 receptors form stable trimers: a novel structural motif of ligand-gated ion channels. *Embo J.* 1998; 17:3016–3028. [PubMed: 9606184]
- Pelegriin P, Surprenant A. Pannexin-1 mediates large pore formation and interleukin-1beta release by the ATP-gated P2X7 receptor. *Embo J.* 2006; 25:5071–5082. [PubMed: 17036048]

- Priel A, Silberberg SD. Mechanism of ivermectin facilitation of human P2X4 receptor channels. *J Gen Physiol.* 2004; 123:281–293. [PubMed: 14769846]
- Ralevic V, Burnstock G. Receptors for purines and pyrimidines. *Pharmacol Rev.* 1998; 50:413–492. [PubMed: 9755289]
- Rassendren F, Buell G, Newbolt A, North RA, Surprenant A. Identification of amino acid residues contributing to the pore of a P2X receptor. *Embo J.* 1997; 16:3446–3454. [PubMed: 9218787]
- Samways DS, Egan TM. Acidic amino acids impart enhanced Ca²⁺ permeability and flux in two members of the ATP-gated P2X receptor family. *J Gen Physiol.* 2007; 129:245–256. [PubMed: 17325195]
- Samways DS, Migita K, Li Z, Egan TM. On the role of the first transmembrane domain in cation permeability and flux of the ATP-gated P2X2 receptor. *J Biol Chem.* 2008; 283:5110–5117. [PubMed: 18048351]
- Silberberg SD, Chang TH, Swartz KJ. Secondary structure and gating rearrangements of transmembrane segments in rat P2X4 receptor channels. *J Gen Physiol.* 2005; 125:347–359. [PubMed: 15795310]
- Silberberg SD, Li M, Swartz KJ. Ivermectin interaction with transmembrane helices reveals widespread rearrangements during opening of P2X receptor channels. *Neuron.* 2007; 54:263–274. [PubMed: 17442247]
- Torres GE, Egan TM, Voigt MM. Topological analysis of the ATP-gated ionotropic [correction of ionotropic P2X2 receptor subunit. *FEBS Lett.* 1998; 425:19–23. [PubMed: 9540999]
- Torres GE, Egan TM, Voigt MM. Identification of a domain involved in ATP-gated ionotropic receptor subunit assembly. *J Biol Chem.* 1999; 274:22359–22365. [PubMed: 10428806]
- Valera S, Hussy N, Evans RJ, Adami N, North RA, Surprenant A, Buell G. A new class of ligand-gated ion channel defined by P2X receptor for extracellular ATP. *Nature.* 1994; 371:516–519. [PubMed: 7523951]
- Vial C, Roberts JA, Evans RJ. Molecular properties of ATP-gated P2X receptor ion channels. *Trends Pharmacol Sci.* 2004; 25:487–493. [PubMed: 15559251]
- Wilkinson WJ, Jiang LH, Surprenant A, North RA. Role of ectodomain lysines in the subunits of the heteromeric P2X2/3 receptor. *Mol Pharmacol.* 2006; 70:1159–1163. [PubMed: 16840712]
- Yan Z, Liang Z, Tomic M, Obsil T, Stojilkovic SS. Molecular determinants of the agonist binding domain of a P2X receptor channel. *Mol Pharmacol.* 2005; 67:1078–1088. [PubMed: 15632318]
- Yan Z, Li S, Liang Z, Tomic M, Stojilkovic SS. The P2X7 receptor channel pore dilates under physiological ion conditions. *J Gen Physiol.* 2008; 132:563–573. [PubMed: 18852304]
- Young MT, Pelegrin P, Surprenant A. Amino acid residues in the P2X7 receptor that mediate differential sensitivity to ATP and BzATP. *Mol Pharmacol.* 2007; 71:92–100. [PubMed: 17032903]

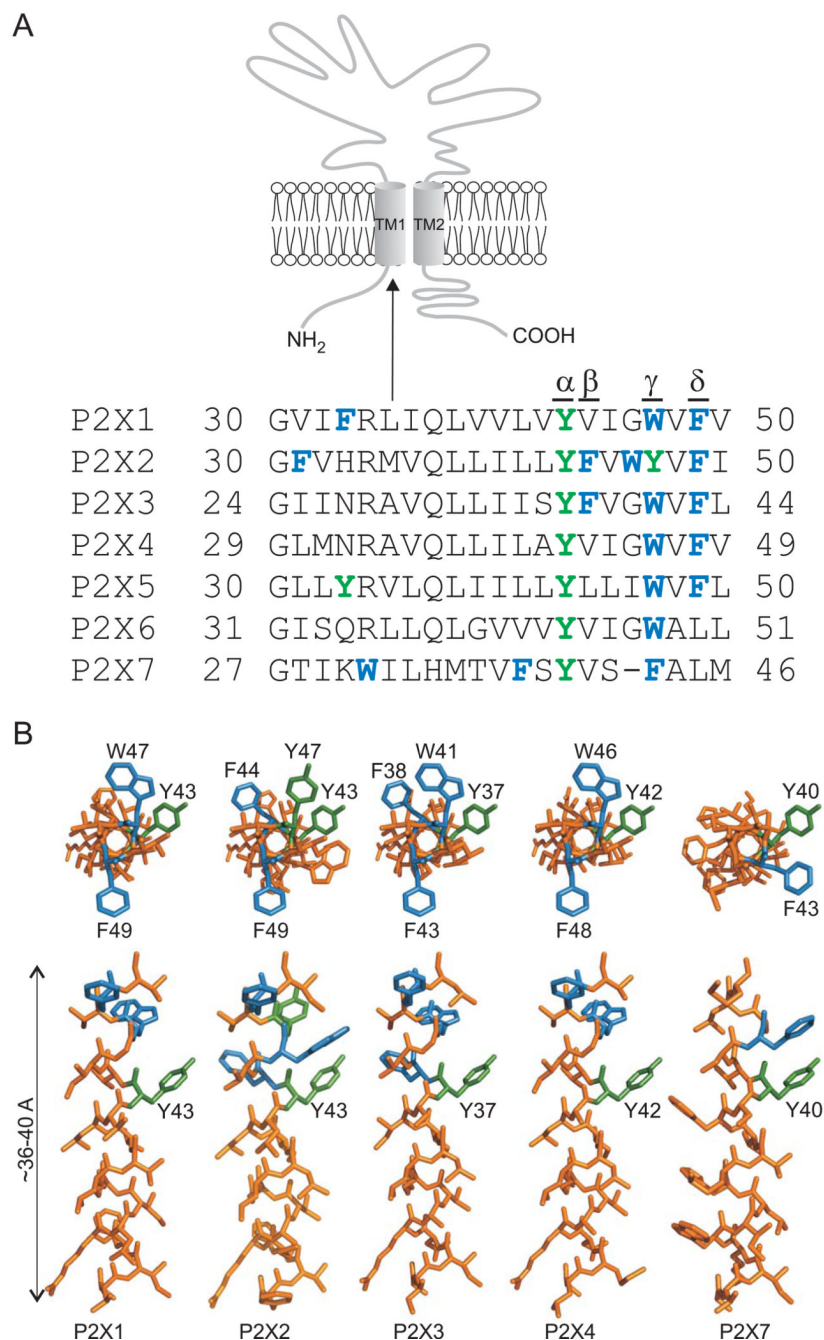


FIGURE 1. Positions of aromatic residues in the TM1 domains of rat P2XRs

(A) Schematic representation of the P2X receptor subunit (*top*) and alignment of amino acid sequences of the first transmembrane domain (*bottom*) of seven rat P2X receptors (P2X1-7). Aromatic residues are shown in *green* (polar) and *blue* (nonpolar). α - δ indicate the positions of the aromatic residues in the upper part of TM1 domain that were studied. (B) Three-dimensional models of predicted α -helical TM1 segments of P2X1R, P2X2R, P2X3R, P2X4R, and P2X7R. The models started with the Gly²⁹ residue and ended with the Val⁴⁹ residue (P2X4 receptor numbering). Helical models viewed from the extracellular side (*top*) and from the membrane (*bottom*) with aromatic residues in the α - δ positions (*green* and *blue*) are shown. This model was generated using PyMol v0.99 (<http://www.pymol.org>).

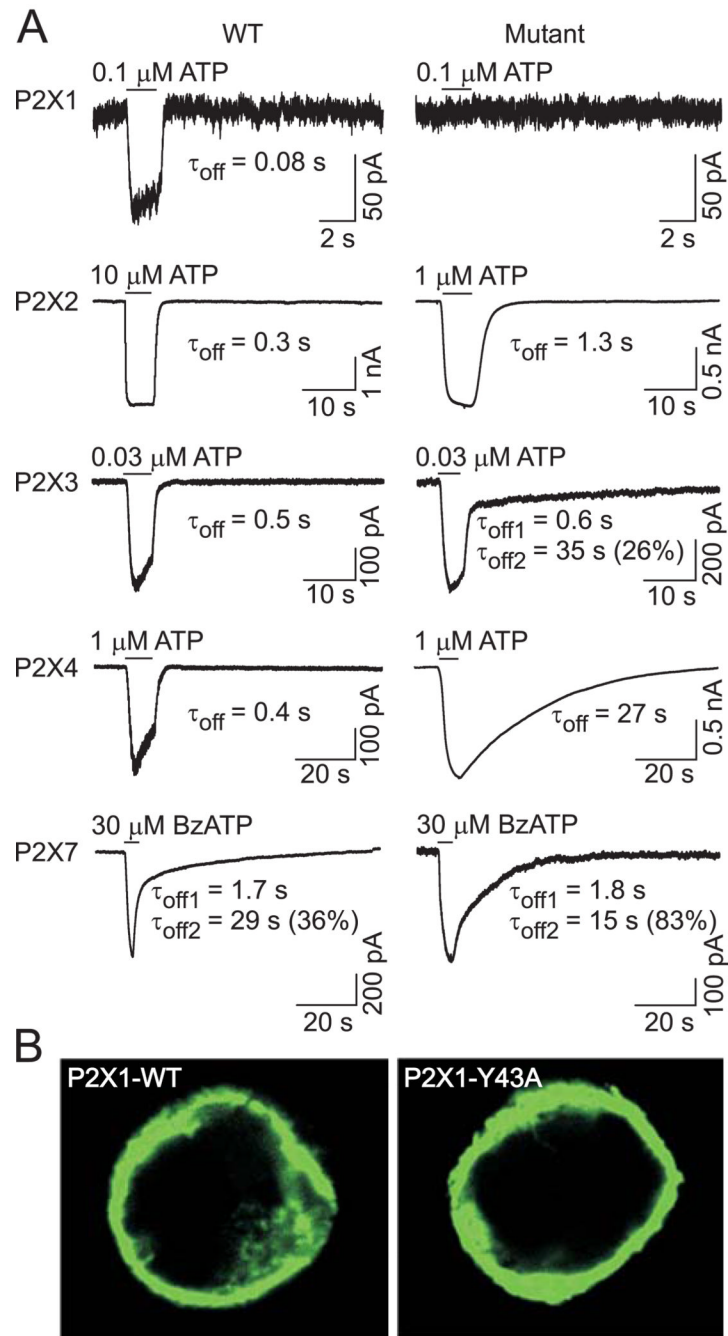


FIGURE 2. Effects of replacement of the conserved TM1 tyrosine residue with alanine on the expression and function of P2XRs

(A) Example records of agonist-induced currents in cells expressing the wild type (WT, *left*) and α -position alanine mutants (*right*) of the P2X1R, P2X2R, P2X3R, P2X4R, and P2X7R. Currents were recorded from HEK293 cells using whole-cell patch clamp recording at a holding potential of -60 mV. Horizontal bars indicate the time of ATP or BzATP application. Numbers below the traces show deactivation time constant (τ_{off}) values derived from mono-exponential fitting of current decay for the P2X1R, P2X2R, and P2X4R and bi-exponential fitting for the P2X3R and P2X7R; for the latter, the percentage of the slow

component ($\tau_{\text{off}2}$) contribution to the current decay is also shown. (B) Expression pattern of the WT and non-functional P2X1R-Y43A mutant in HEK293 cells.

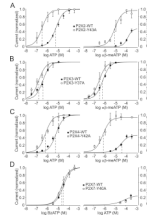


FIGURE 3. Effects of replacement of the conserved TM1 tyrosine residue with alanine on the potency of agonists for P2XRs

Concentration response curves to agonists in WT (closed circles) and TM1 tyrosine to alanine mutants (open circles) of P2XRs expressed in HEK293 cells. (*Left*) Increase in the sensitivity of the P2X2R (A), P2X3R (B), and P2X4R (C) mutants to ATP and the lack of effects of TM1-Tyr mutation on the sensitivity of P2X7R receptors to BzATP (D). (*Right*) A leftward shift in the sensitivity of TM1-Tyr mutants of P2X2R (A), P2X3R (B), and P2X4R (C) to $\alpha\beta$ -meATP and the lack of effects of this mutation on the sensitivity of P2X7R to ATP (D). Vertical dashed lines indicate the EC_{50} value, and mean \pm SEM values are shown in Table 2. Each concentration was examined in between five and 30 different cells and current responses were normalized to an averaged maximum current induced by 100 μ M ATP for the P2X2R, P2X3R, and P2X4R and 300 μ M BzATP for the P2X7R.

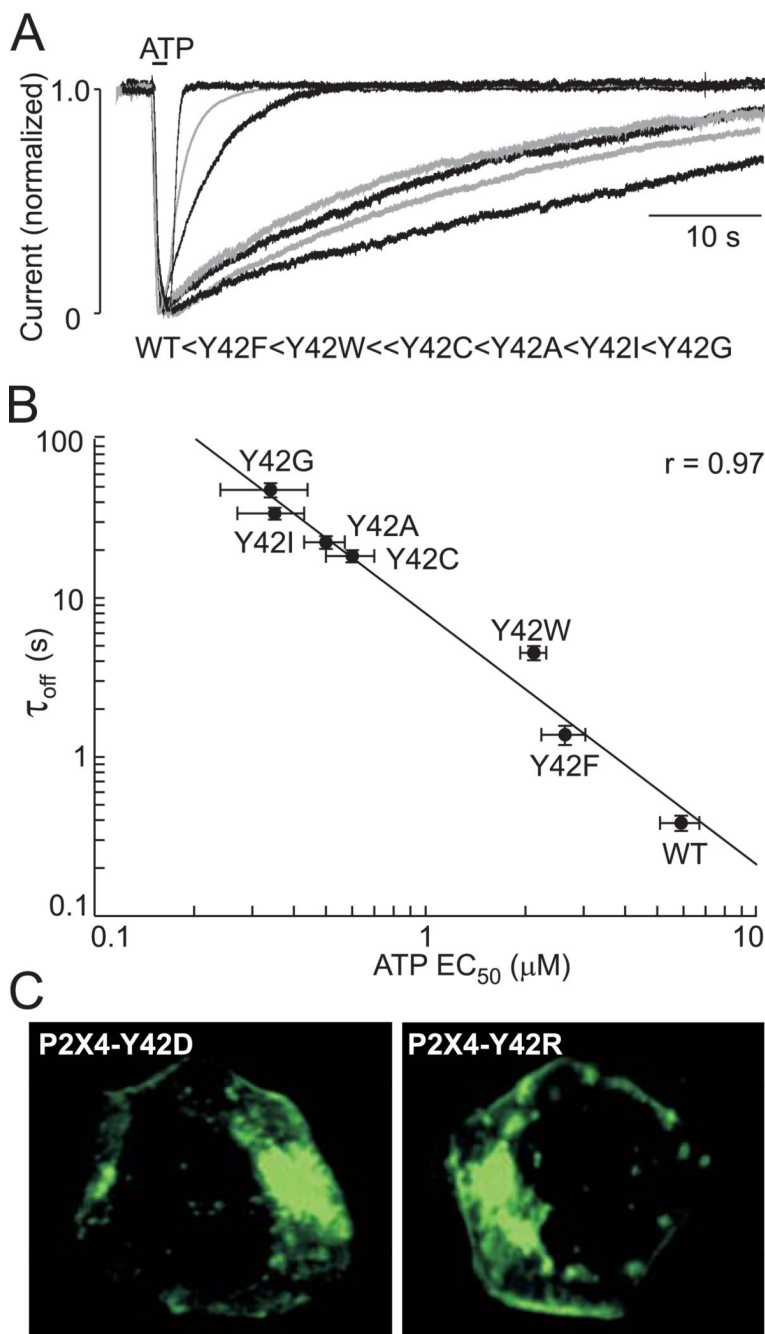


FIGURE 4. Partial rescue of receptor function by replacement of the P2X4R-Tyr⁴² residue with phenylalanine and tryptophan

(A) Effects of replacement of the P2X4R-Tyr⁴² residue with alanine, isoleucine, cysteine, glycine, phenylalanine, tryptophan, aspartate, or glutamate on the rates of receptor deactivation. Superimposed responses to ATP (0.3–1 μM) of WT and functional mutants are shown. The order of the deactivation time constants for current decay after ATP removal is shown below the traces. (B) Logarithmic relationship between the EC_{50} values for ATP and deactivation time constants for functional P2X4R-Tyr⁴² mutants. (C) The expression pattern of non-functional EGFP-tagged P2X4-Y42D and P2X4-Y42R mutants in HEK293 cells.

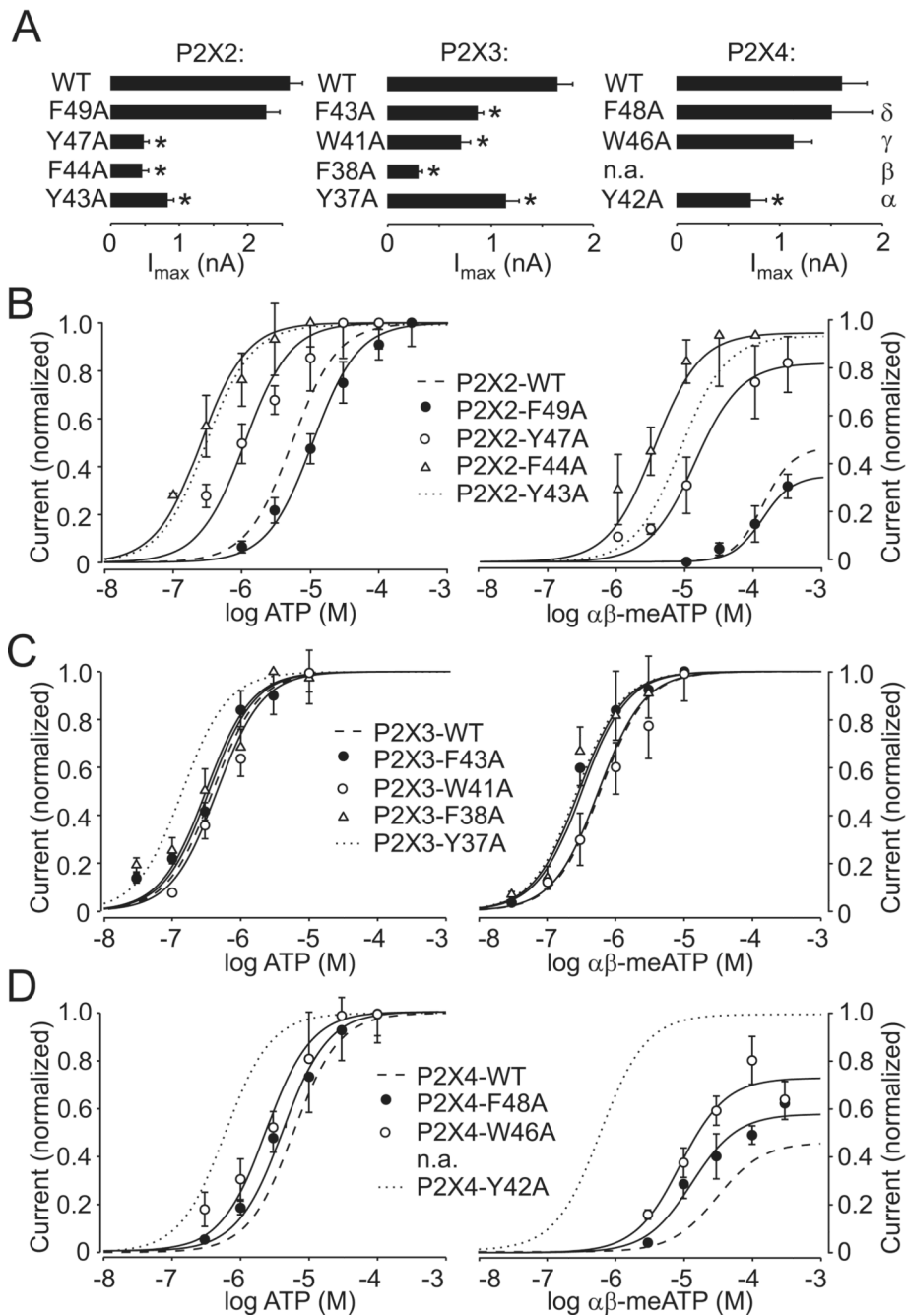


FIGURE 5. Characterization of the TM1 aromatic residue P2XR mutants

(A) Comparison of maximum current amplitudes stimulated by supramaximal ATP concentrations in cells expressing the WT and mutant P2X2aR, P2X3R, and P2X4R. (B–D) Dose-response curves for ATP (*left*) and $\alpha\beta$ -meATP (*right*) in cells expressing aromatic residue mutants of the P2X2a (B), P2X3R (C), and P2X4R (D). The $\alpha\beta$ -meATP efficacy was measured by comparison with the maximum effect of ATP.

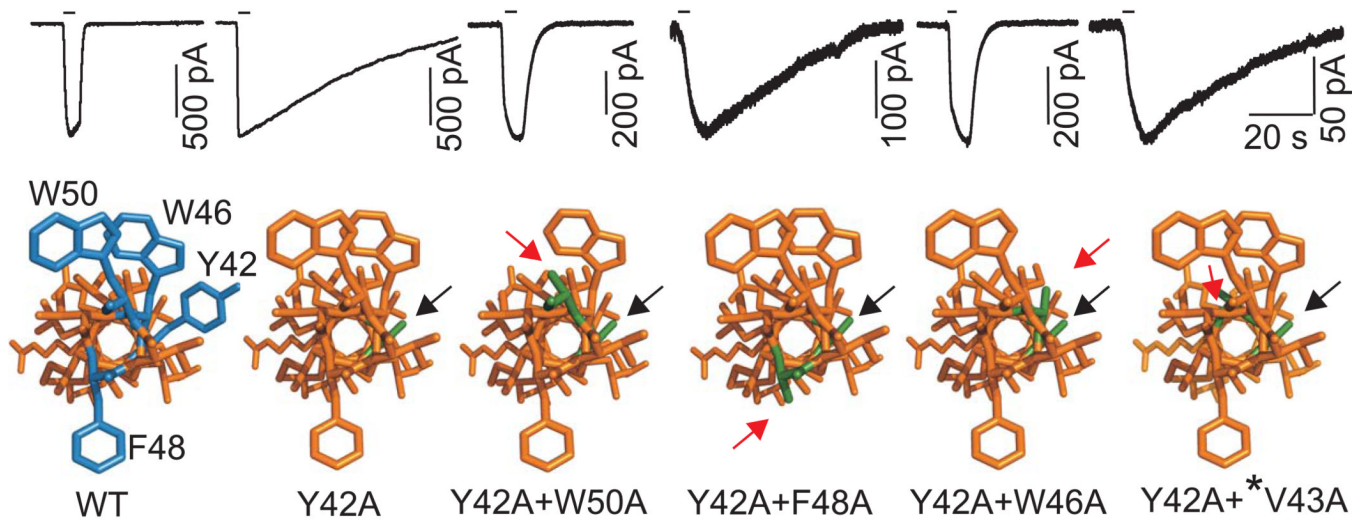


FIGURE 6. Replacement of ipsilateral but not contralateral TM1 aromatic residues with alanine restores P2X4R function

Time-courses of currents from the P2X4R-WT and single- and double-point alanine mutants in response to brief 1 μM ATP application (indicated by horizontal bars; *top*) and dependence of receptor deactivation on the position of the substituted residues in a helical model of the P2X4R (*bottom*). Helical models of P2X4R are viewed from the extracellular side with aromatic residues in the 42, 46, 48 and 50 positions (*blue*) and their alanine substitutions (*green*). *Black arrows* indicate alanine substitution of the conserved tyrosine, and *red arrows* indicate the second alanine substitution of another aromatic (Trp⁴⁶, Trp⁵⁰ and Phe⁴⁸) residue or non-aromatic residue Val⁴³ (*) present in the β position.

TABLE 1

Effects of single- and double-point alanine mutagenesis of aromatic residues in the upper part of P2XR-TM1 domains on receptor functions.

P2XRs	ATP EC ₅₀ (μM)	ATP I _{max} (nA)	ATP τ _{off} (s)	αβ-meATP EC ₅₀ (μM)	αβ-meATP efficacy (%) ^a
P2X2R-WT	5.4±0.8	2.6±0.2	0.34±0.05	>100	44
P2X2R-F49A	10.8±2.1*	2.2±0.2	0.44±0.06	>100	32
P2X2R-Y47A	0.82±0.1*	0.46±0.1*	0.36±0.02	11.8±2*	83
P2X2R-F44A	0.26±0.05*	0.44±0.1*	1±0.07*	3.4±1*	95
P2X2R-Y43A	0.28±0.05*	0.80±0.1*	1.3±0.1*	8.2±1*	94
P2X2R-Y43F	8.2±1.8	2.8±0.4	0.47±0.1	>100	65
P2X3R-WT	0.35±0.12	1.6±0.2	0.55±0.05	0.59±0.1	100
P2X3R-F43A	0.35±0.2	0.9±0.1*	0.75±0.06	0.32±0.2	100
P2X3R-W41A	0.39±0.15	0.7±0.07*	0.67±0.08	0.56±0.15	100
P2X3R-F38A	0.31±0.2	0.3±0.05*	1.95±0.27*	0.29±0.05	100
P2X3R-Y37A	0.14±0.1*	1.2±0.2	0.60±0.01 34±2* ^b	0.27±0.1	100
P2X4R-WT	4.6±0.3	1.6±0.2	0.42±0.03	57±9	42
P2X4R-W50A	5.1±1.3	1.7±0.2	0.35±0.08	85±15	24
P2X4R-F48A	4.1±0.5	1.5±0.8	0.6±0.04	13.4±2.1*	62
P2X4R-W46A	3.0±0.5	1.0±0.16	0.6±0.1	8.9±1.6*	73
P2X4R-Y42A	0.6±0.1*	0.6±0.3*	24±2.9*	0.6±0.05*	100
P2X4R-42A+V43A	0.9±0.1*	0.3±0.03*	49±2.6*	0.9±0.3*	100
P2X4R-42A+W46A	1.4±0.2*	1.4±0.3	1.2±0.05*	4.7±2.0*	44
P2X4R-42A+F48A	0.3±0.1*	0.2±0.03*	54±5*	0.3±0.1*	100
P2X4R-42A+W50A	1.6±0.3*	1.2±0.4	1.6±0.2*	8.3±2.3*	53
P2X4R-Y42A+I39A	n.d.	0.1±0.05*	n.d.	n.d.	n.d.
P2X4R-42A+V35A	0.6±0.1*	0.4±0.1*	33±4.4*	0.6±0.2*	100

P2XRs	ATP EC ₅₀ (μM)	ATP I _{max} (nA)	ATP τ _{off} (s)	αβ-meATP EC ₅₀ (μM)	αβ-meATP efficacy (%) ^a
P2X4R-42A+G29A	0.4±0.1*	0.5±0.1*	34±3.4*	0.4±0.05*	77

Data shown are mean±SEM values derived from 5 to 35 cells.

(*) P<0.01 between WT and mutants

^a αβ-me ATP efficacy was calculated as ratio of I_{max} at 300 μM αβ-meATP/I_{max} at 100 μM ATP

^b deactivation kinetics of this mutant was biexponential and τ_{off2} value for slow deactivation component contributed with 36±4 % to the current decay.